



Computational Simulation of the High Strain Rate Tensile Response of Polymer Matrix Composites

Robert K. Goldberg
Glenn Research Center, Cleveland, Ohio

The NASA STI Program Office . . . in Profile

Since its founding, NASA has been dedicated to the advancement of aeronautics and space science. The NASA Scientific and Technical Information (STI) Program Office plays a key part in helping NASA maintain this important role.

The NASA STI Program Office is operated by Langley Research Center, the Lead Center for NASA's scientific and technical information. The NASA STI Program Office provides access to the NASA STI Database, the largest collection of aeronautical and space science STI in the world. The Program Office is also NASA's institutional mechanism for disseminating the results of its research and development activities. These results are published by NASA in the NASA STI Report Series, which includes the following report types:

- **TECHNICAL PUBLICATION.** Reports of completed research or a major significant phase of research that present the results of NASA programs and include extensive data or theoretical analysis. Includes compilations of significant scientific and technical data and information deemed to be of continuing reference value. NASA's counterpart of peer-reviewed formal professional papers but has less stringent limitations on manuscript length and extent of graphic presentations.
- **TECHNICAL MEMORANDUM.** Scientific and technical findings that are preliminary or of specialized interest, e.g., quick release reports, working papers, and bibliographies that contain minimal annotation. Does not contain extensive analysis.
- **CONTRACTOR REPORT.** Scientific and technical findings by NASA-sponsored contractors and grantees.

- **CONFERENCE PUBLICATION.** Collected papers from scientific and technical conferences, symposia, seminars, or other meetings sponsored or cosponsored by NASA.
- **SPECIAL PUBLICATION.** Scientific, technical, or historical information from NASA programs, projects, and missions, often concerned with subjects having substantial public interest.
- **TECHNICAL TRANSLATION.** English-language translations of foreign scientific and technical material pertinent to NASA's mission.

Specialized services that complement the STI Program Office's diverse offerings include creating custom thesauri, building customized data bases, organizing and publishing research results . . . even providing videos.

For more information about the NASA STI Program Office, see the following:

- Access the NASA STI Program Home Page at <http://www.sti.nasa.gov>
- E-mail your question via the Internet to help@sti.nasa.gov
- Fax your question to the NASA Access Help Desk at 301-621-0134
- Telephone the NASA Access Help Desk at 301-621-0390
- Write to:
NASA Access Help Desk
NASA Center for Aerospace Information
7121 Standard Drive
Hanover, MD 21076



Computational Simulation of the High Strain Rate Tensile Response of Polymer Matrix Composites

Robert K. Goldberg
Glenn Research Center, Cleveland, Ohio

Prepared for the
14th Symposium on Composite Materials: Testing and Design
sponsored by the American Society for Testing and Materials
Pittsburgh, Pennsylvania, March 11–12, 2002

National Aeronautics and
Space Administration

Glenn Research Center

Acknowledgments

The author would like to acknowledge Fiberite, Inc. for providing the material used for the experimental tests on the IM7/977-2 system along with additional information and data. The author would also like to acknowledge Prof. Amos Gilat of Ohio State University for conducting the tensile tests presented in this report.

Trade names or manufacturers' names are used in this report for identification only. This usage does not constitute an official endorsement, either expressed or implied, by the National Aeronautics and Space Administration.

Available from

NASA Center for Aerospace Information
7121 Standard Drive
Hanover, MD 21076

National Technical Information Service
5285 Port Royal Road
Springfield, VA 22100

Available electronically at <http://gltrs.grc.nasa.gov/GLTRS>

Computational Simulation of the High Strain Rate Tensile Response of Polymer Matrix Composites

Robert K. Goldberg
National Aeronautics and Space Administration
Glenn Research Center
Cleveland, Ohio 44135

Summary

A research program is underway to develop strain rate dependent deformation and failure models for the analysis of polymer matrix composites subject to high strain rate impact loads. Under these types of loading conditions, the material response can be highly strain rate dependent and nonlinear. State variable constitutive equations based on a viscoplasticity approach have been developed to model the deformation of the polymer matrix. The constitutive equations are then combined with a mechanics of materials based micromechanics model which utilizes fiber substructuring to predict the effective mechanical and thermal response of the composite. To verify the analytical model, tensile stress-strain curves are predicted for a representative composite over strain rates ranging from around 1×10^{-5} /sec to approximately 400/sec. The analytical predictions compare favorably to experimentally obtained values both qualitatively and quantitatively. Effective elastic and thermal constants are predicted for another composite, and compared to finite element results.

Introduction

NASA Glenn Research Center has an ongoing research program to investigate the feasibility of developing jet engine fan containment systems composed of polymer matrix composite materials. To design such a system, the ability to correctly predict the nonlinear, strain rate dependent deformation and failure of the composite under high strain rate loading conditions is required. The deformation of polymer composites is ordinarily assumed to be independent of strain rate and linearly elastic [1]. However, researchers such as Daniel, et. al [2] and Staab and Gilat [3] have shown experimentally that the elastic properties of polymer matrix composites do indeed vary with strain rate. Furthermore, for applications such as a fan containment system, composites with toughened polymer matrices are likely to be used, which could contribute to a nonlinear deformation behavior for the composite. Researchers such as Thiruppukuzhi and Sun [4] have analyzed the nonlinear deformation of polymer matrix composites on the macroscopic level using plasticity and viscoplasticity theory. Previous efforts by the author of this report [5] have utilized simplified micromechanics techniques to analyze the nonlinear, rate dependent deformation of polymer matrix composites at relatively low strain rates.

The objective of the current paper is to simulate the strain rate dependent tensile deformation of a representative polymer matrix composite with varying fiber orientations at strain rates ranging from around 1×10^{-5} /sec to approximately 400/sec. An analytical

model will be presented in which state variable constitutive equations based on viscoplasticity theory are utilized to predict the strain rate dependent response of the polymer matrix, including a preliminary method of accounting for the effects of hydrostatic stresses. The micromechanics techniques used to predict the effective mechanical and thermal response of the composite will be described. In the micromechanics method presented here, the unit cell is divided into a number of horizontal slices, and uniform stress and uniform strain assumptions are then applied to each slice to obtain the effective stresses, elastic and thermal constants, and effective inelastic strains for each slice. Laminate theory is then applied to obtain the effective properties and response for each lamina, and then applied again to obtain the effective response for the composite laminate. Finally, verification studies will be discussed in which tensile stress-strain curves of a representative polymer matrix composite are generated analytically using the mathematical model, and the results will be compared to experimentally obtained values. Furthermore, effective elastic and thermal constants will be computed for a second representative composite and the results will be compared to values obtained using finite element analyses.

Polymer Constitutive Equations

Polymers are known to have a strain rate dependent deformation response that is nonlinear above about one or two percent strain. For this study, the Ramaswamy-Stouffer viscoplastic state variable model [6], which was originally developed to analyze the viscoplastic deformation of metals above one-half of the melting temperature, has been modified to simulate the rate dependent inelastic deformation of polymers. There is some physical motivation in utilizing constitutive equations that were developed to model viscoplastic metals to analyze the deformation response of polymer matrix materials. For example, the “yield stress” in polymers and the “saturation stress” in metals have both been defined as the stress level in a uniaxial tension test where the applied strain rate equals the inelastic strain rate [6,7]. In state variable constitutive equations, a single unified strain variable is defined to represent all inelastic strains. Furthermore, there is no defined yield stress. Inelastic strains are assumed to be present at all values of stress, only very small in the “elastic” range of deformation. State variables, which evolve with stress and inelastic strain, are defined to represent the average effects of the deformation mechanisms.

Several limitations and assumptions have been specified in the development of the constitutive equations. Temperature effects are neglected. The nonlinear strain recovery observed in polymers on unloading is not simulated, and phenomena such as creep, relaxation and high cycle fatigue are not accounted for in the equations.

In the modified Ramaswamy-Stouffer model, the components of the inelastic strain rate tensor, $\dot{\epsilon}_{ij}^I$, are defined as a function of the deviatoric stress components, s_{ij} , and the components of the tensorial internal stress state variable tensor Ω_{ij} in the form

$$\dot{\epsilon}_{ij}^I = D_o \exp \left[-\frac{1}{2} \left(\frac{Z_o^2}{3K_2} \right)^n \right] \left(\frac{s_{ij} - \Omega_{ij}}{\sqrt{K_2}} \right) \quad (1)$$

where D_o , Z_o , and n are material constants. D_o is a material constant which represents the maximum inelastic strain rate, Z_o is a material constant which represented the initial, isotropic “hardness” of the material before any load is applied and n is a material constant which controls the rate dependence of the deformation response. The term K_2 is defined as follows

$$K_2 = \frac{1}{2} (s_{ij} - \Omega_{ij}) (s_{ij} - \Omega_{ij}) \quad (2)$$

and represents the second invariant of the overstress tensor. The elastic components of strain are added to the inelastic strain to obtain the total strain. The following relation defines the internal stress state variable rate

$$\dot{\Omega}_{ij} = \frac{2}{3} q \Omega_m \dot{\epsilon}_{ij}^I - q \Omega_{ij} \dot{\epsilon}_e^I \quad (3)$$

where q is a material constant that represents the “hardening” rate, Ω_m is a material constant that represents the maximum value of the internal stress, and ϵ_e^I is the effective inelastic strain. The internal stress is assumed to be equal to zero when the material is in its virgin state.

The material constants that need to be determined include D_0 , n , Z_0 , Ω_m , and q . The procedure for determining the values of these constants is summarized here. Further details can be found in Stouffer and Dame [6] and Goldberg [5]. The constants are determined using stress-strain curves obtained from a set of uniaxial constant strain rate tensile tests of the polymer matrix material. Each test is conducted at a different total strain rate. A basic assumption is that the constants determined from uniaxial tensile tests are valid under multiaxial stress conditions and can be used in Equation 1. The value of D_0 is currently assumed to be equal to a value of 10^4 times the maximum expected total strain rate, which correlates with the maximum possible inelastic strain rate. To determine the values of n , Z_0 , and Ω_m , Equation 1 is simplified into its uniaxial representation to model the results of the constant strain rate uniaxial tensile tests and rearranged into an appropriate form. Data pairs of the total strain rate and saturation stress (yield stress) values from each of the tensile stress-strain curves are taken. Values for Ω_m are estimated for the material, with initial estimates ranging from 50% to 75% of the highest saturation stress found to work well. For each strain rate, the data values are substituted into the rearranged form of Equation 1, and represent a point on a master curve. The number of points in the master curve equal the number of strain rates at which tensile tests were conducted. A least squares regression analysis is then performed on the master curve to determine the required constants. The value for Ω_m is adjusted until an optimal fit to the data is obtained.

To determine the value for q for Equation 3, first the equation is converted into its uniaxial equivalent and integrated. At saturation (yield), the value of the internal stress is assumed to approach the maximum value, and the integrated equation is solved for q . If the inelastic strain at saturation is found to vary with strain rate, the parameter q is computed at each strain rate and regression techniques are utilized to determine an expression for the variation of q .

One key difference between the deformation response of polymers and the deformation response of metals is that the mean stress effects in polymers are significant, and need to be dealt with in a constitutive model. Bordonaro [8] indicated a possible way of accounting for the effects of hydrostatic stresses in a state variable constitutive model was to modify the effective stress terms. In this work, pressure dependence is included by multiplying the shear terms in the K_2 invariant in Equation 2 by the correction factor

$$\alpha = \left(\frac{\sigma_m}{\sqrt{J_2}} \right)^\beta \quad (4)$$

where σ_m is the mean stress, J_2 is the second invariant of the deviatoric stress tensor, and β is a material constant. The value of the parameter β is currently determined empirically by fitting data from composites with shear dominated fiber orientations, such as $[\pm 45^\circ]_s$. Efforts are currently underway to account for the hydrostatic stress effects in a more systematic manner, based on using polymer tensile and shear data.

Composite Micromechanical Model

Micromechanics techniques are used to predict the effective properties and deformation response of the individual plies in the composite laminate based on the constituent properties. Laminate theory is then used to compute the effective deformation response of the entire composite. The unit cell is defined to consist of a single fiber and its surrounding matrix. Due to symmetry, only one-quarter of the unit cell was analyzed. The composites are assumed to have a periodic, square fiber packing and a perfect interfacial bond is specified. Classical laminate theory is assumed to apply to the composites considered for this study, and each lamina is considered to be in a state of plane stress. In certain applications, the out-of-plane stresses in the lamina could be significant, in which case classical laminate theory would not apply. However, in order to simplify the mathematics in the analysis, and since the plane stress assumption is commonly made in the analysis of composite laminates, for this study any out-of-plane effective stresses are neglected. If these stresses are eventually determined to be significant, a three-dimensional laminate theory could be applied to allow for the presence of transverse pressures and transverse shear stresses. The fibers are assumed to be transversely isotropic and linearly elastic with a circular cross-section. The matrix is assumed to be isotropic, with a rate dependent, nonlinear deformation response computed using the equations described in the previous section. A key assumption of this approach is that the in-situ matrix properties are equivalent to the bulk properties of the polymer. However, the advantage of using this type of methodology is that it is simpler to conduct experiments on the pure resin and to determine the material constants from the pure resin data as opposed to trying to back out the resin properties from composite test data. Furthermore, a key goal of this research is to provide a methodology that facilitates reducing the amount of testing of the composite that is required to obtain strain rate dependent material properties that can be input into a finite element code. Conducting strain rate dependent tensile tests on the pure resin and using that data to predict the composite deformation response is also much simpler than conducting tests on the

composite. However, if in comparing test data obtained from composite specimens to analytical predictions it appears that the bulk matrix properties do not accurately reflect the in-situ state of the matrix, the polymer properties can always be appropriately adjusted.

In previous work [5], the portion of the unit cell that was analyzed was divided into four rectangular subcells, one for the fiber and three matrix subcells, similar to Aboudi's Method of Cells [9]. By applying uniform stress and uniform strain assumptions to the subcells within the unit cell, a system of ten coupled simultaneous equations resulted which were solved for the stresses in each subcell. The effective elastic constants and inelastic strains for the composite lamina were also determined.

In order to obtain more accurate results, the ability to refine the unit cell to allow for a larger number of subcells is desirable. However, by applying the approach used previously, solving a large number of simultaneous equations would be required to obtain the subcell stresses. The number of equations would increase as the number of subcells increased.

However, by considering the approximations required for classical laminate theory, since each ply must be in a global state of plane stress one could assume that each row of subcells in the unit cell must be in a state of plane stress. While the out-of-plane stresses could be nonzero in individual subcells, the effective volume average of the stresses for each row of subcells would equal zero. If transverse pressures and transverse shear stresses are not neglected, the effective out-of-plane stresses in each row of subcells would be a non-zero constant value throughout the thickness of the unit cell. However, for this study only in-plane stresses are assumed to be present. By assuming a constant out-of-plane stress in each row of subcells in the unit cell model, the behavior of each row of subcells can be decoupled. One can divide the unit cell up into an arbitrary number of horizontal slices (rows). A schematic demonstrating the fiber substructuring is shown in Figure 1. Uniform stress and uniform strain assumptions can then be applied to each slice to obtain the subslice (subcells within a slice) stresses, as well as the effective inelastic strains and effective elastic constants for the slice. Laminate theory can then be used to obtain the effective elastic and thermal constants and effective inelastic strains for the composite lamina, and then applied again to obtain the effective elastic constants and force resultants due to inelastic strains for the laminate. Similar approaches have been used by Whitney [10] and Greszczuk [11] to determine the elastic constants of polymer matrix composites. Mital, Murthy and Chamis [12] applied a slicing approach to determine the elastic properties and deformation response of ceramic matrix composites.

The significance of this approach is that the stresses for each slice (both subslice and effective) can be determined independently, which significantly reduces the number of simultaneous equations that need to be solved. Furthermore, no matter how many slices are included in the model, the size of the system of equations for each slice remains constant. Therefore, instead of solving one large set of simultaneous equations, multiple small sets of equations can be solved, which reduces the complexity of the problem.

Slicing Algorithm

The unit cell is divided up into several rectangular horizontal slices. The portion of the unit cell that contains fiber and matrix is divided up into an odd number of slices of equal thickness. The remaining matrix areas on the top and bottom of the unit cell are

contained in individual slices. In Figure 1, the unit cell is divided up into five fiber slices, and the portion of the unit cell that is analyzed (analysis cell) is divided up into three fiber slices. The unit cell is assumed to measure one unit in length by one unit in height, and the analysis cell is assumed to measure 0.5 units in length by 0.5 units in height. The fiber slices are of equal thickness, except for the bottom slice in the analysis cell which is one-half as thick as the remaining fiber slices due to symmetry. The slicing algorithm used is very similar to that used by Mital, et al. [12].

To compute the fiber volume ratio and thickness ratio (the ratio of slice thickness to total analysis cell thickness) for each slice in the analysis cell, the following procedure is followed. The first step is to compute the area of the cross-section of the fiber within each slice. The overall diameter of the fiber (d_f) is related to the fiber volume fraction of the overall composite (V_f) through the following relationship

$$d_f = \sqrt{\frac{4V_f}{\pi}} \quad (5)$$

and this term can be used along with the standard geometric definition of the radius of a circle to compute the horizontal coordinate of any point on the outer surface of the fiber in terms of the fiber volume fraction and the vertical coordinate. The area of the portion of the fiber contained within each slice (A_f^i) can be computed by integrating the resulting expression between the vertical (z) coordinates of the top and bottom of slice “i”

$$A_f^i = \int_{z_{i-1}}^{z_i} \sqrt{\frac{V_f}{\pi} - z^2} dz \quad (6)$$

which is also the equivalent area of the rectangular fiber slice in the analysis cell.

The fiber volume fraction of each slice composed of fiber and matrix is equal to the fiber area in each slice divided by the total slice area (the slice thickness multiplied by 0.5). The thickness ratio for each slice composed of both fiber and matrix is equal to the slice thickness divided by 0.5, the assumed total height of the analysis cell. The fiber volume fraction of the top slice consisting of matrix only is equal to zero, and the thickness ratio of the top slice is equal to one minus the sum of the thickness ratio of the remaining slices.

Slice Micromechanics Equations

The effective properties, effective inelastic strains and effective thermal strains of each slice are computed independently. The responses of each slice are combined using laminate theory to obtain the effective response of the corresponding lamina. Most of the slices are assumed to have two subslices, one subslice composed of fiber material and one subslice composed of matrix material. The top slice is assumed to be composed of matrix material only. The micromechanics equations are for those slices composed of both fiber and matrix material. The stresses in the slices composed of pure matrix can be computed using the matrix elastic properties and inelastic constitutive equations. The standard transversely isotropic compliance matrix (or isotropic in the case of the matrix)

is used to relate the local strains to the local stresses in the fiber and matrix. Each slice is assumed to be in a state of plane stress on the global level, but out-of-plane normal stresses can exist in each subslice.

Along the fiber direction (direction 11), the strains are assumed to be uniform in each subslice, and the stresses are combined using volume averaging. The in-plane transverse normal stresses (22 direction) and the in-plane shear stresses (12 direction) are assumed to be uniform in each subslice, and the strains are combined using volume averaging. The out-of-plane strains (33 direction) are assumed to be uniform in each subslice. The volume average of the out-of-plane stresses in each subslice is assumed to be equal to zero, enforcing a plane stress condition on the global level for the slice.

The orthotropic compliance matrix is used to relate the strains (ϵ_{ij}) to the stresses (σ_{ij}) in each constituent, using the following relations

$$\begin{Bmatrix} \epsilon_{11} \\ \epsilon_{22} \\ \epsilon_{33} \end{Bmatrix} = \begin{bmatrix} S_{11} & S_{12} & S_{13} \\ S_{12} & S_{22} & S_{23} \\ S_{13} & S_{23} & S_{33} \end{bmatrix} \begin{Bmatrix} \sigma_{11} \\ \sigma_{22} \\ \sigma_{33} \end{Bmatrix} + \begin{Bmatrix} \epsilon'_{11} \\ \epsilon'_{22} \\ \epsilon'_{33} \end{Bmatrix} + \begin{Bmatrix} \alpha_{11} \\ \alpha_{22} \\ \alpha_{33} \end{Bmatrix} \Delta T \quad (7)$$

$$\gamma_{12} = S_{66} \sigma_{12} + 2\epsilon'_{12} \quad (8)$$

where α_{11} , α_{22} , and α_{33} are the coefficients of thermal expansion, ΔT is the change in temperature and ϵ'_{ij} are the inelastic strains. Note that in these equations S_{ij} represents the components of the compliance matrix, not the components of the deviatoric stress tensor s_{ij} as in the previous section. Also note that engineering shear strains (γ_{ij}) are used in the analysis.

The addition of the inelastic strain components to the standard orthotropic elastic constitutive law facilitates the incorporation of inelasticity into the constitutive relations. For the fiber, which is assumed to be linear elastic, these components are neglected. For the fiber, which is transversely isotropic, S_{13} is set equal to S_{12} and S_{33} is set equal to S_{22} . For the matrix material, which is assumed to be isotropic, S_{23} and S_{13} are set equal to S_{12} , and S_{22} and S_{33} are set equal to S_{11} . Furthermore, α_{33} is set equal to α_{22} for the fiber and α_{33} and α_{22} are set equal to α_{11} for the matrix.

By combining the uniform stress and uniform strain assumptions with the constituent stress-strain relations, the following system of equations results

$$\begin{aligned} \epsilon_{11} - \frac{S_{12f}}{S'} \epsilon'_{33m} - \left[\frac{S_{12f}(\alpha_m - \alpha_{22f})}{S'} + \alpha_{11f} \right] \Delta T &= \left[S_{11f} - \frac{S_{12f}^2}{S'} \right] \sigma_{11f} + \left[\frac{S_{12f} S_{12m}}{S'} \right] \sigma_{11m} + \\ &\left[S_{12f} + \frac{S_{12f}(S_{12m} - S_{23f})}{S'} \right] \sigma_{22} \end{aligned} \quad (9)$$

$$\begin{aligned} \varepsilon_{11} - \varepsilon'_{11m} + V' \frac{S_{12m}}{S'} \varepsilon'_{33m} + \left[V' \frac{S_{12m}(\alpha_m - \alpha_{22f})}{S'} - \alpha_m \right] \Delta T = \\ V' \left[\frac{S_{12f} S_{12m}}{S'} \right] \sigma_{11f} + \left[S_{11m} - V' \frac{S_{12m}^2}{S'} \right] \sigma_{11m} + \left[S_{12m} - V' \frac{S_{12m}(S_{12m} - S_{23f})}{S'} \right] \sigma_{22} \end{aligned} \quad (10)$$

$$\begin{aligned} \varepsilon_{22} - (1 - V_f) \varepsilon'_{22m} - \frac{V_f (S_{23f} - S_{12m})}{S'} \varepsilon'_{33m} - \\ \left[V_f \alpha_{22f} + (1 - V_f) \alpha_m + V_f \frac{(S_{23f} - S_{12m})(\alpha_m - \alpha_{22f})}{S'} \right] \Delta T = \\ V_f \left[S_{12f} - \frac{S_{12f}(S_{23f} - S_{12m})}{S'} \right] \sigma_{11f} + \left[(1 - V_f) S_{12m} + \frac{V_f S_{12m}(S_{23f} - S_{12m})}{S'} \right] \sigma_{11m} \\ + \left[V_f S_{22f} + (1 - V_f) S_{11m} + V_f (S_{23f} - S_{12m}) \frac{S_{12m} - S_{23f}}{S'} \right] \sigma_{22} \end{aligned} \quad (11)$$

$$\gamma_{12} = [V_f S_{66f} + (1 - V_f) S_{66m}] \sigma_{12} + 2(1 - V_f) \varepsilon'_{12m} \quad (12)$$

$$S' = S_{22f} + S_{11m} V' \quad (13)$$

$$V' = \frac{V_f}{1 - V_f} \quad (14)$$

that can be solved for the unknown stresses in the subslices. The total strains and subslice inelastic strains are considered to be the known values in solving this problem. The subscript “f” is used to denote fiber related properties, and the subscript “m” is used to denote matrix related properties. Stresses and strains with no subscript are used to represent effective stresses and strains for the slice (not the composite ply or laminate). The symbol “ V_f ” is used here to represent the fiber volume ratio for the slice, computed using the methods discussed earlier, not the total fiber volume fraction for the composite.

By substituting the subslice stresses back into the equations defining the uniform stress assumptions, an expression relating the effective stresses to the effective strains in the slice is obtained

$$\begin{Bmatrix} \sigma_{11} \\ \sigma_{22} \\ \sigma_{12} \end{Bmatrix} = \begin{bmatrix} Q_{11} & Q_{12} & 0 \\ Q_{21} & Q_{22} & 0 \\ 0 & 0 & Q_{66} \end{bmatrix} \begin{Bmatrix} \varepsilon_{11} \\ \varepsilon_{22} \\ \gamma_{12} \end{Bmatrix} - \begin{Bmatrix} e_1 \\ e_2 \\ e_3 \end{Bmatrix} - \begin{Bmatrix} a_1 \\ a_2 \\ 0 \end{Bmatrix} \quad (15)$$

where $[Q_{ij}]$ represents the effective plane stress stiffness matrix for the slice, $\{e_i\}$ represents the stress resultants due to inelastic strains and $\{a_i\}$ represents the stress resultants due to thermal strains. To compute the effective inelastic strains and effective

thermal expansion coefficients for the slice, the $\{e_i\}$ and $\{a_i\}$ vectors are brought to the left hand side of Equation 15 and the expression is solved for the total strains. The effective inelastic strains for the slice can be computed using the following expression

$$\begin{Bmatrix} \varepsilon'_{11} \\ \varepsilon'_{22} \\ \gamma'_{12} \end{Bmatrix} = \begin{bmatrix} S_{11} & S_{12} & 0 \\ S_{21} & S_{22} & 0 \\ 0 & 0 & S_{66} \end{bmatrix} \begin{Bmatrix} e_1 \\ e_2 \\ e_3 \end{Bmatrix} \quad (16)$$

where $[S_{ij}]$ is the effective compliance matrix for the slice, and $\{\varepsilon'_{ij}\}$ represents the effective inelastic strain vector for the slice. Similarly, the effective thermal expansion coefficients for the slice can be computed using the following expression

$$\begin{Bmatrix} \alpha_{11} \\ \alpha_{22} \end{Bmatrix} = \begin{bmatrix} S_{11} & S_{12} \\ S_{21} & S_{22} \end{bmatrix} \begin{Bmatrix} a_1 \\ a_2 \end{Bmatrix} \frac{1}{\Delta T} \quad (17)$$

where α_{11} and α_{22} are the effective thermal expansion coefficients for the slice.

To compute the effective stiffness matrix, effective thermal expansion coefficients and effective inelastic strains for the lamina (which are equivalent to the equivalent properties for the analysis cell) from the effective stiffness matrix, thermal expansion coefficients, and inelastic strains for each slice, the following procedure is used. First, the in-plane strains for each slice are assumed to be constant and equal to the in-plane strains for the lamina. The total in-plane stresses for the lamina are assumed to be equal to the volume average of the in-plane stresses for each slice, as follows

$$\begin{Bmatrix} \sigma_{11} \\ \sigma_{22} \\ \sigma_{12} \end{Bmatrix}_l = \sum_{i=1}^{N_f+1} \begin{Bmatrix} \sigma_{11} \\ \sigma_{22} \\ \sigma_{12} \end{Bmatrix}_i h_f^i \quad (18)$$

where N_f is the number of fiber slices in the analysis cell, $\{\sigma_{ij}\}_l$ are the effective stresses in the lamina, h_f^i represents the thickness ratio of each slice as defined earlier, and the summation is over all of the slices (i).

To compute the plane stress stiffness matrix and effective inelastic strains for the lamina, Equation 15 for the slice is rewritten as

$$\begin{Bmatrix} \sigma_{11} \\ \sigma_{22} \\ \sigma_{12} \end{Bmatrix} = \begin{bmatrix} Q_{11} & Q_{12} & 0 \\ Q_{21} & Q_{22} & 0 \\ 0 & 0 & Q_{66} \end{bmatrix} \begin{Bmatrix} \varepsilon_{11} - \varepsilon'_{11} - \alpha_{11}\Delta T \\ \varepsilon_{22} - \varepsilon'_{22} - \alpha_{22}\Delta T \\ \gamma_{12} - \gamma'_{12} \end{Bmatrix} \quad (19)$$

where Equation 16 is applied to compute the $\{\varepsilon'_{ij}\}$ vector from the $\{e_i\}$ vector and Equation 17 is applied to compute the thermal expansion coefficients from the a_i vector. By substituting Equation 19 into Equation 18, the effective plane stress stiffness matrix for the lamina, $[Q_{jk}]_l$, is obtained as follows

$$[Q_{jk}]_l = \sum_{i=1}^{N_f+1} [Q_{jk}]_i h_f^i \quad (20)$$

where the summation is again over all of the slices. Likewise, by following the same procedures used to go from Equation 15 to Equation 16, the following expression is obtained for computing the effective inelastic strains for the lamina

$$\begin{Bmatrix} \varepsilon_{11}^I \\ \varepsilon_{22}^I \\ \gamma_{12}^I \end{Bmatrix}_l = \begin{bmatrix} S_{11} & S_{12} & 0 \\ S_{21} & S_{22} & 0 \\ 0 & 0 & S_{66} \end{bmatrix}_l \sum_{i=1}^{N_f+1} \begin{bmatrix} Q_{11} & Q_{12} & 0 \\ Q_{21} & Q_{22} & 0 \\ 0 & 0 & Q_{66} \end{bmatrix}_i \begin{Bmatrix} \varepsilon_{11}^I \\ \varepsilon_{22}^I \\ \gamma_{12}^I \end{Bmatrix}_i h_f^i \quad (21)$$

where $\{\varepsilon_{ij}^I\}_l$ is the effective inelastic strain vector for the lamina and $[S_{ij}]_l$ is the effective compliance matrix for the lamina. A similar procedure is used to compute the effective thermal expansion coefficients for the lamina. By applying laminate theory again, the effective response of the composite laminate can be computed as has been described in Goldberg [13].

Simulation of Strain Rate Dependent Tensile Deformation

To verify the micromechanics equations, a series of analyses have been carried out using a representative polymer matrix composite system that exhibits a strain rate dependent, nonlinear deformation response. The material examined, supplied by Fiberite, Inc., consists of carbon IM7 fibers in a 977-2 toughened epoxy matrix. Longitudinal tensile tests have been conducted on the neat resin and composite laminates with various fiber orientations at The Ohio State University. Tests were conducted at strain rates of about 5×10^{-5} /sec, about 1.0/sec and about 400–600/sec. Dog-bone shaped specimens were used with a gage length of approximately 0.9525 cm. The low strain rate testing was conducted using an Instron hydraulic testing machine. The high strain rate tests were conducted using a tensile split Hopkinson bar apparatus.

The IM7/977-2 composite has a fiber volume ratio of 0.60. The material properties used in this study for the IM7 fiber include a longitudinal modulus of 276 GPa, a transverse modulus of 12.4 GPa, a longitudinal Poisson's ratio of 0.25, a transverse Poisson's ratio of 0.25 and an in-plane shear modulus of 20.0 GPa. The longitudinal modulus, longitudinal Poisson's ratio and in-plane shear modulus are as given in Gates, et al. [14]. The transverse modulus of the fiber was reduced slightly from the value given in Gates, et al. [14] in order to provide a good correlation in the elastic range with data from $[90^\circ]$ specimens. Since the transverse modulus given in Gates, et al. [14] was also a correlated value, a variation of this sort was considered acceptable. The value for the transverse Poisson's ratio was taken from Murthy, et al. [15] based on representative carbon fiber data. Temperature effects and processing related issues were not accounted for in the current analyses due to the lack of available data. Temperature effects might be incorporated into the predictions in the future.

The material properties for the 977-2 resin were determined using the procedures described earlier. Note that since this resin did not reach a "saturation" stress before

failure, appropriate values were extrapolated from the tensile data and used to obtain the material properties. The value for the constant “ β ” required for the correction factor given in Equation 4 was determined to be strain rate dependent. In addition, the material constant “ q ” from Equation 3 was found to be rate dependent for this material. The elastic modulus for the matrix at high strain rates was found to be significantly higher than the modulus at the low and moderate strain rates. The value of the constant “ q ” was found to be quite low at high strain rates. This variation is most likely due to the fact that in metals, for which the polymer constitutive equations used here were originally developed, the elastic modulus is assumed not to vary with strain rate. However, for the polymer examined here the modulus increased significantly at high strain rates. This would lead to a significant increase in the inelastic strain at saturation compared to the lower strain rates, which would lead to a reduction in the value of “ q ”. The values of the material constants for the 977-2 resin include an elastic modulus of 3.52 GPa for the low and moderate strain rates and 13.8 GPa for the high strain rate, a Poisson’s ratio of 0.40, and inelastic constants as follows: $D_0=1\times 10^6$, $n=0.42$, $Z_0=2180$ MPa, q ranging from 85 for the low strain rate, 160 for the moderate strain rate and 20 for the high strain rate, $\Omega_m=76$ MPa, and β ranging from 1.05 for the low strain rate, 0.90 for the moderate strain rate and 0.50 for the high strain rate.

Experimental and computed longitudinal tensile stress-strain curves for two laminate configurations ($[45^\circ]$ and $[\pm 45^\circ]_s$) of the IM7/977-2 material are shown in Figure 2 and Figure 3. These laminate configurations were chosen due the pronounced nonlinearity and strain rate dependence observed in the experimental results. Three fiber slices were used in the analysis cell for the computations. This value was found to yield sufficiently converged answers. In Figure 2, results for the $[45^\circ]$ laminates at strain rates of 4.75×10^{-5} /sec, 1.2/sec and 405/sec are shown. In Figure 3, results for the $[\pm 45^\circ]_s$ laminates at strain rates of 9×10^{-5} /sec, 2.1/sec and 604/sec are shown. As can be seen in the figures, the analytical model captures the rate dependence and nonlinearity of the experimental stress-strain curves. Furthermore, the comparison between the experimental and computed results is quite good.

Prediction of Effective Elastic and Thermal Constants

To validate the ability of the composite micromechanics to predict the effective elastic and thermal properties of a polymer matrix composite, the initial, elastic, room temperature material properties of a representative carbon fiber reinforced polymer matrix composite with a $[0^\circ]$ fiber orientation were computed. The results are compared to values obtained through finite element analyses by Hyer [16]. For the carbon fiber, the longitudinal modulus is taken to be 233 GPa, the transverse modulus is taken to be 23.1 GPa, the longitudinal Poisson’s ratio is 0.20, the transverse Poisson’s ratio is 0.40, the in-plane shear modulus is 8.96 GPa, the longitudinal coefficient of thermal expansion is -0.540×10^{-6} /K, and the transverse coefficient of thermal expansion is 10.10×10^{-6} /K. For the matrix, the modulus is 4.62 GPa, the Poisson’s ratio is 0.36 and the coefficient of thermal expansion is 41.4×10^{-6} /K. The fiber volume ratio was set to 0.60. All of the properties are as given by Hyer [16]. For the analysis, three fiber slices were once again used in the analysis cell.

The predicted values of the longitudinal (E_{11}) and transverse (E_{22}) modulus, longitudinal Poisson's ratio (ν_{12}), in-plane shear modulus (G_{12}), and longitudinal (α_{11}) and transverse (α_{22}) thermal expansion coefficients are listed in Table 1 along with the values computed using finite element analyses [16]. For the thermal expansion coefficients, values computed using a micromechanics approach based on energy methods [1] are also listed. As can be seen in the table, the elastic properties computed using the methodology presented in this paper match the finite element results quite well. The predicted thermal expansion coefficients differ slightly from the finite element results. However, the current methodology provides an improved prediction in the longitudinal direction when compared to the energy based method, and an equivalent prediction in the transverse direction. Overall, the current methodology provides good predictions of effective elastic and thermal properties of polymer matrix composites.

Table 1- *Prediction of Effective Material Properties*

| Property | Finite Element | Energy Method | Predicted |
|--------------------|----------------|---------------|-----------|
| E_{11} (GPa) | 141.7 | ----- | 141.7 |
| E_{22} (GPa) | 12.4 | ----- | 12.6 |
| ν_{12} | 0.259 | ----- | 0.266 |
| G_{12} (GPa) | 4.05 | ----- | 3.90 |
| α_{11} (/K) | 0.088 | 0.007 | 0.112 |
| α_{22} (/K) | 26.4 | 28.5 | 29.1 |

Conclusions

An analytical model has been developed to analyze the strain rate dependent, nonlinear deformation response of polymer matrix composites. State variable constitutive equations based on the Ramaswamy-Stouffer model are used to compute the deformation response of the polymer matrix. A mechanics of materials based micromechanics method in which the unit cell was divided into several slices is used to predict the effective elastic and thermal properties and the effective deformation of the composite. The stress strain curves computed using the analytical model compared favorably to the experimental results across the entire range of strain rates, indicating that the analysis is correctly capturing the important features of the deformation response. Effective elastic and thermal properties were also correctly predicted using the analytical model. The analytical methods described in this study can be used in explicit finite element codes to provide a more realistic analysis of deformation during blade-out events for fan containment systems composed of composite materials.

Future efforts will concentrate on improving the methodology used to account for mean stress effects in the polymer constitutive equations. The ability to account for thermal effects will also be added to the constitutive equations. The micromechanics will be modified to allow for the analysis of woven and braided composites.

References

- [1] Daniel, I.M., *Engineering Mechanics of Composite Materials*, Oxford University Press, New York, 1994.
- [2] Daniel, I.M., Hamilton, W.G., and LaBedz, R.H., “Strain Rate Characterization of Unidirectional Graphite/Epoxy Composite,” *Composite Materials: Testing and Design (Sixth Conference) ASTM STP 787*, I.M. Daniel, Ed., American Society for Testing and Materials, West Conshohocken, PA, 1982, pp. 393–413.
- [3] Staab, G.H. and Gilat, A., “High Strain Rate Response of Angle-Ply Glass/Epoxy Laminates,” *Journal of Composite Materials*, Vol. 29, 1995, pp. 1308–1320.
- [4] Thiruppukuzhi, S.V. and Sun, C.T., “Testing and modeling high strain rate behavior of polymeric composites,” *Composites Part B*, Vol. 29B, 1998, pp. 535–546.
- [5] Goldberg, R.K., “Strain Rate Dependent Deformation and Strength Modeling of a Polymer Matrix Composite Utilizing a Micromechanics Approach”, NASA/TM—1999-209768, National Aeronautics and Space Administration, Washington, D.C., December 1999.
- [6] Stouffer, D.C. and Dame, L.T., *Inelastic Deformation of Metals: Models, Mechanical Properties and Metallurgy*, John Wiley and Sons, New York, 1996.
- [7] Ward, I.M., *Mechanical Properties of Solid Polymers*, John Wiley and Sons, New York, 1983.
- [8] Bordonaro, C.M., “Rate Dependent Mechanical Behavior of High Strength Plastics: Experiment and Modeling,” PhD Dissertation, Rensselaer Polytechnic Institute, Troy, New York, 1995.
- [9] Aboudi, J., *Mechanics of Composite Materials: A Unified Micromechanical Approach*, Elsevier, New York, 1991.
- [10] Whitney, J.M., “A Laminate Analogy for Micromechanics,” *Proceedings of the American Society for Composites Eighth Technical Conference*, G. Newaz, Ed., Technomic Publishing Company, Inc., Lancaster, PA, 1993, pp. 785–794.
- [11] Greszczuk, L.B., “Interfiber Stresses in Filamentary Composites,” *AIAA Journal*, Vol. 9, 1971, pp. 1274–1280.
- [12] Mital, S.K., Murthy, P.L.N., and Chamis, C.C., “Micromechanics for Ceramic Matrix Composites Via Fiber Substructuring,” *Journal of Composite Materials*, Vol. 29, 1995, pp. 614–633.

- [13] Goldberg, R.K., "Implementation of Laminate Theory Into Strain Rate Dependent Micromechanics Analysis of Polymer Matrix Composites," NASA/TM—2000-210351, National Aeronautics and Space Administration, Washington, D.C., August 2000.
- [14] Gates, T.S., Chen, J.-L., and Sun, C.T., "Micromechanical Characterization of Nonlinear Behavior of Advanced Polymer Matrix Composites," *Composite Materials: Testing and Design (Twelfth Volume) ASTM STP 1274*, R.B. Deo and C.R. Saff, Eds., American Society for Testing and Materials, West Conshohocken, PA, 1996, pp. 295–319.
- [15] Murthy, P.L.N., Ginty, C.A., and Sanfeliz, J.G., "Second Generation Integrated Composite Analyzer (ICAN) Computer Code," NASA TP–3290, National Aeronautics and Space Administration, Washington, D.C., January 1993.
- [16] Hyer, M.W., *Stress Analysis of Fiber Reinforced Composite Materials*, McGraw-Hill, New York, 1998.

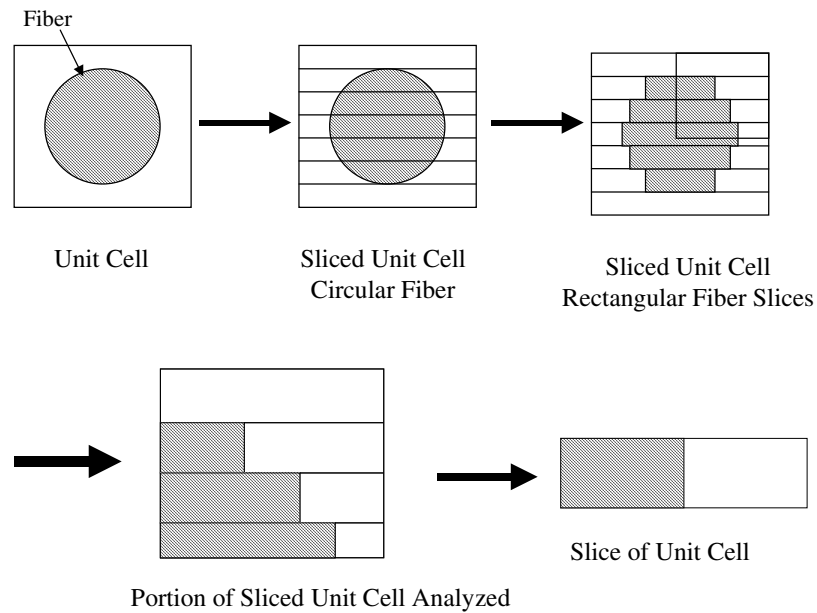


Figure 1 - Schematic showing relationship between unit cell and slices for micromechanics.

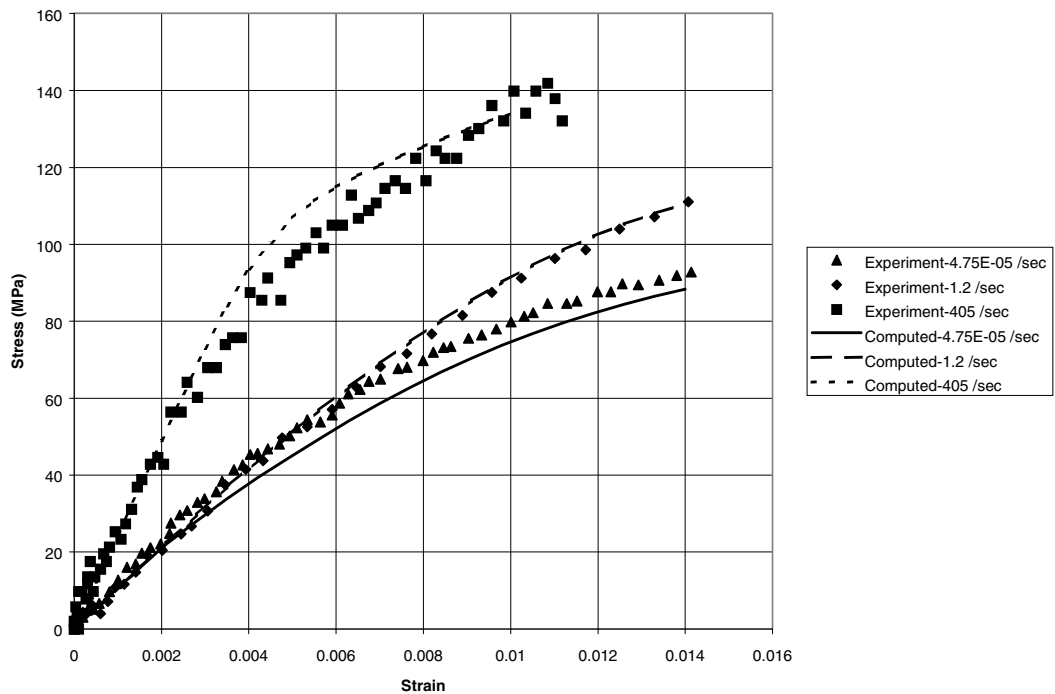


Figure 2 - Experimental and computed results for IM7/977-2 [45°] laminates at strain rates of 4.75×10^{-5} /sec, 1.2/sec and 405/sec.

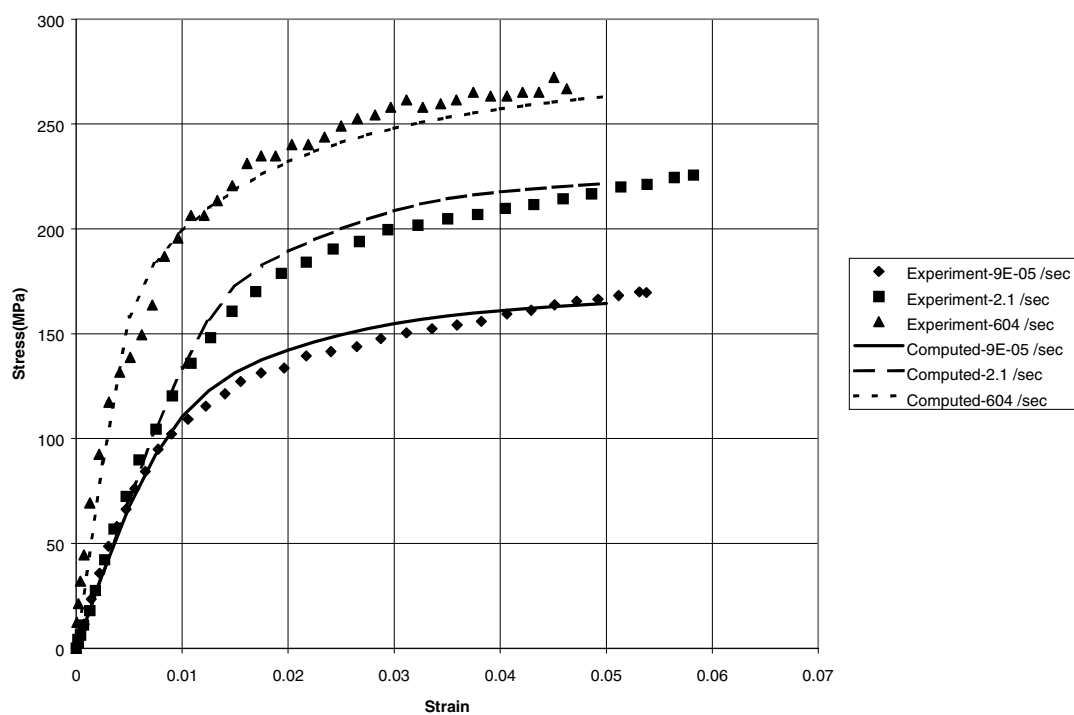


Figure 3 - *Experimental and computed results for IM7/977-2 $[\pm 45^\circ]_s$ laminates at strain rates of 9×10^{-5} /sec, 2.1/sec and 604/sec*

| REPORT DOCUMENTATION PAGE | | | Form Approved OMB No. 0704-0188 | |
|--|---|--|--|--|
| Public reporting burden for this collection of information is estimated to average 1 hour per response, including the time for reviewing instructions, searching existing data sources, gathering and maintaining the data needed, and completing and reviewing the collection of information. Send comments regarding this burden estimate or any other aspect of this collection of information, including suggestions for reducing this burden, to Washington Headquarters Services, Directorate for Information Operations and Reports, 1215 Jefferson Davis Highway, Suite 1204, Arlington, VA 22202-4302, and to the Office of Management and Budget, Paperwork Reduction Project (0704-0188), Washington, DC 20503. | | | | |
| 1. AGENCY USE ONLY (Leave blank) | | 2. REPORT DATE March 2002 | | 3. REPORT TYPE AND DATES COVERED Technical Memorandum |
| 4. TITLE AND SUBTITLE Computational Simulation of the High Strain Rate Tensile Response of Polymer Matrix Composites | | | 5. FUNDING NUMBERS WU-708-24-13-00 | |
| 6. AUTHOR(S) Robert K. Goldberg | | | | |
| 7. PERFORMING ORGANIZATION NAME(S) AND ADDRESS(ES) National Aeronautics and Space Administration John H. Glenn Research Center at Lewis Field Cleveland, Ohio 44135-3191 | | | 8. PERFORMING ORGANIZATION REPORT NUMBER E-13257 | |
| 9. SPONSORING/MONITORING AGENCY NAME(S) AND ADDRESS(ES) National Aeronautics and Space Administration Washington, DC 20546-0001 | | | 10. SPONSORING/MONITORING AGENCY REPORT NUMBER NASA TM-2002-211489 | |
| 11. SUPPLEMENTARY NOTES Prepared for the 14th Symposium on Composite Materials: Testing and Design sponsored by the American Society for Testing and Materials, Pittsburgh, Pennsylvania, March 11-12, 2002. Responsible person, Robert K. Goldberg, organization code 5920, 216-433-3330. | | | | |
| 12a. DISTRIBUTION/AVAILABILITY STATEMENT Unclassified - Unlimited Subject Category: 24 Available electronically at http://gltrs.grc.nasa.gov/GLTRS This publication is available from the NASA Center for AeroSpace Information, 301-621-0390. | | | 12b. DISTRIBUTION CODE | |
| 13. ABSTRACT (Maximum 200 words) A research program is underway to develop strain rate dependent deformation and failure models for the analysis of polymer matrix composites subject to high strain rate impact loads. Under these types of loading conditions, the material response can be highly strain rate dependent and nonlinear. State variable constitutive equations based on a viscoplasticity approach have been developed to model the deformation of the polymer matrix. The constitutive equations are then combined with a mechanics of materials based micromechanics model which utilizes fiber substructuring to predict the effective mechanical and thermal response of the composite. To verify the analytical model, tensile stress-strain curves are predicted for a representative composite over strain rates ranging from around 1×10^{-5} /sec to approximately 400/sec. The analytical predictions compare favorably to experimentally obtained values both qualitatively and quantitatively. Effective elastic and thermal constants are predicted for another composite, and compared to finite element results. | | | | |
| 14. SUBJECT TERMS Polymer matrix composites; Micromechanics; Viscoplasticity; Stain rate; Constitutive equations; Impact | | | 15. NUMBER OF PAGES 22 | |
| | | | 16. PRICE CODE | |
| 17. SECURITY CLASSIFICATION OF REPORT Unclassified | 18. SECURITY CLASSIFICATION OF THIS PAGE Unclassified | 19. SECURITY CLASSIFICATION OF ABSTRACT Unclassified | 20. LIMITATION OF ABSTRACT | |